Journal of Materials Chemistry C

Programmed twisting of phenylene-ethynylene linkages from aromatic stacking interactions

Journal:	*Journal of Materials Chemistry C*
Manuscript ID	TC-ART-11-2018-005612.R1
Article Type:	Paper
Date Submitted by the Author:	04-Dec-2018
Complete List of Authors:	Mullin, William; Tufts University, Chemistry Pawle, Robert; Tufts University, Chemistry Sharber, Seth; Tufts University, Chemistry Mueller, Peter; MIT, Chemistry Thomas, Samuel; Tufts University, Chemistry

Journal Name

ARTICLE

Programmed twisting of phenylene-ethynylene linkages from aromatic stacking interactions

Received 00th January 20xx,
Accepted 00th January 20xx

DOI: 10.1039/x0xx00000x

www.rsc.org/

William J. Mullin,[a] Robert H. Pawle,[a] Seth A. Sharber,[a] Peter Müller,[b] and Samuel W. Thomas III*[a]

Control over the conformation and packing of conjugated materials is an unsolved problem that prevents rational design for organic optoelectronics, such as preventing self-quenching of luminescent molecules. Exacerbating this challenge is a general lack of widely applicable strategies for controlling packing with discrete, directional non-covalent interactions. Here we present a series of conjugated molecules with diverse backbones of three or four arenes that feature pentafluorobenzyl ester substituents. Nearly all the compounds reveal intramolecular stacking interactions between the fluoroarene (ArF) side-chains and non-fluorinated arenes (ArH) in the middles of the chromophores; a twisted PE linkage accompanies each example of this intramolecular ArF-ArH stacking. Furthermore, these molecules can resist dramatic changes to emission upon transition from organic solution to thin film when the ArF prevent interchromophore interactions. By broadening the structural space of conjugated backbones over which ArF-ArH stacking can twist PE linkages reliably and prevent self-quenching of solids with simple synthetic approaches, this work suggests fluorobenzyl 2-ethynyl benzoates as a supramolecular synthon in the crystal engineering of organic optoelectronic materials.

Introduction

Conjugated small molecules are important components of organic electronic devices that enable tuning of optoelectronic properties with changes of chemical structure.[1] Among the expanding panoply of conjugated moieties, phenylene ethynylenes (PEs) are well-established yet unique molecules that possess backbones of alternating arenes and triple bonds. Solid-state PEs have applications in sensing,[2-4] anti-microbial coatings,[5-7] nanoelectronics,[8-10] and photovoltaic cells.[11-13] These compounds adopt wide ranges of conformations along their conjugated backbones due to low barriers of rotation, which can be as small as 1 kcal/mol.[14,15] Although this shallow energy surface makes controlling solid-state conformations and luminescence challenging, it also presents opportunities for responsive materials, as the optoelectronic properties of conjugated molecules depend strongly on conformation.[16-18]

Several approaches exist for controlling PE backbone conformations via modifications to the main chain in order to bias luminescent properties. Covalent tethering between the two arenes in elaborated tolanes can lock twisted conformations to achieve phosphorescence,[19,20] while steric interactions bias PE torsions and prevent intermolecular aggregation.[21,22] Several related strategies use directional non-covalent interactions between moieties installed into PE backbones,[23,24] but that can restrict the types of main-chain arenes that can participate. A notable example is intramolecular hydrogen bonds that increase the co-planarity of PEs in solution.[25] Overall, however, the purposeful integration of discrete, directional non-covalent interactions to engineer solid-state packing of conjugated materials is relatively rare, especially those involving the non-conjugated pendant groups.

The large number arenes present in conjugated materials frequently means that their interactions[26] dictate solid-state packing.[27] While edge-to-face interactions of benzene dimers are electrostatically favorable, the opposing electronic distribution of perfluorinated arenes and non-fluorinated arenes yields cofacial interactions (ArF-ArH stacking) as a generally applicable design motif in crystal engineering.[28,29] These cofacial aromatic interactions present the advantage of easily tunable strengths through Hammett-type electronic substituent effects. Examples of the influence of include fluorinated acenes pentacene[30] and rubrene,[31] which cofacially stack, strongly deviating from the classic "herringbone" packing of acenes that features edge-face interactions.

Our group has used directional ArF-ArH stacking to control both the conformation and packing of solid PEs.[32-34] In this approach, stacking interactions between i) fluorinated benzyl substituents on a central dibenzylterepthalate, and ii) terminal rings of a 3-ring PE facilitate twisting of the PE backbones and prevent chromophore aggregation. In several publications that focus exclusively on this common molecular core (Figure 1), we demonstrated that electronic substituent effects dictate whether stacking interactions occur,[33] as well as tunable

[a] Department of Chemistry, Tufts University, 62 Talbot Ave., Medford, MA 02155, USA; [b] Department of Chemistry, MIT, 77 Massachusetts Ave., Cambridge MA 02139. *Email - sam.thomas@tufts.edu

Electronic Supplementary Information (ESI) available: [NMR spectra, optical spectra, and crystallographic details]. See DOI: 10.1039/x0xx00000x
CCDC 1875124-1875132

reversible mechanofluorochromism based on the lengths of alkyl substituents.[34]

The potential generality of these directional ArF-ArH interactions to control solid-state conformations of PEs, however, remains an open question. Our objective in this work was to broaden the applicability of such stacking interactions between conjugated arenes and pendant fluorinated rings to program twisted PE linkages, and demonstrate such control as an approach to improve the predictability of their solid-state luminescence. To this end, we have incorporated perfluorinated benzyl esters into PEs composed of up to four aromatic rings along their conjugated backbones, with a greater diversity of conjugated chemical linkages beyond alkynes and easily installed terminal rings bearing fluoroarene pendants for intramolecular stacking. These molecules display diverse intermolecular and intramolecular packing as a result of ArF-ArH stacking interactions, and show prominent twisted PE linkages in their crystal structures, which in some cases dictate different solid state optical properties depending on the extent of electronic coupling that the twisting enables.

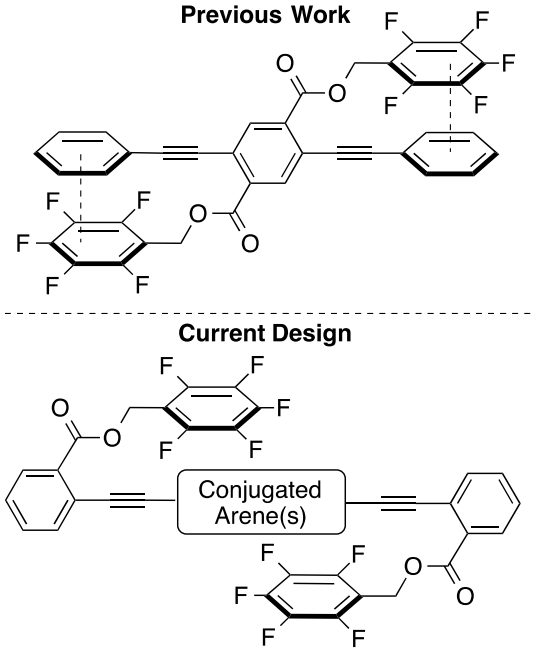

Figure 1. Comparison of general molecular structures in which ArF-ArH stacking interactions twist PE backbones in our previous work (*top*), and the more general design of molecules presented herein (*bottom*).

Experimental Section

All reactants and solvents were purchased from commercial sources and used without further purification. Syntheses requiring air free conditions were performed using standard Schlenk techniques under an argon atmosphere. Flask column chromatography was performed using silica gel (230-400 mesh). NMR spectra were acquired on a Bruker Avance III 500 or a Bruker DPX-300 spectrometer. UV/visible absorbance and fluorescence spectra were acquired for target compounds in dilute chloroform solution and thin films. UV/visible absorbance spectra were acquired with a Varian Cary-100 spectrophotometer, employing quartz cuvettes and glass microscope slides for solution and thin film measurements, respectively. Fluorescence emission and excitation spectra were acquired with a PTI Quantum Master 4 equipped with a 75 W Xe lamp and time-correlated single photon-counting module. Relative quantum yields in dilute solution were determined using quinine sulfate in 0.1 M sulfuric acid and anthracene in ethanol as standards using values reported by Melhuish.[35] Single crystals for X-ray diffraction analysis were grown by evaporation of solvent from chloroform solutions, or from diffusion of hexanes into solution of the compound in chloroform. Single crystal diffraction data were collected on a Bruker D8 Quest diffractometer coupled to a photon CMOS detector with Mo Kα radiation (λ = .71073 Å).

Compounds **1** and **3** were prepared according to a previously reported procedure.[36] A solution of pentafluorobenzyl alcohol or benzyl alcohol (5.25 mmol) in dichloromethane (60 mL) was added to a round bottom flask containing 2-iodobenzoic acid (5 mmol), dimethylaminopyridine (1 mmol), and dicyclohexylcarbodiimide (5.5 mmol). The reaction was stirred for 16 hours at room temperature. The reaction mixture was then filtered over a bed of Celite, and rinsed with diethyl ether. The resulting organic solution was washed with water, brine, dried over $MgSO_4$, filtered, and concentrated *in vacuo*. The crude product was purified by flash column chromatography on silica, using dichloromethane as eluent.

1: Obtained as a colorless solid in 75% yield. ^{1}H NMR (300 MHz, $CDCl_3$): δ 7.98 (d, 1H), 7.7 (d, 1H), 7.34 (t, 1H), 7.16 (t, 1H), 5.44 (s, 2H). ^{13}C NMR (125 MHz, $CDCl_3$): δ 165.6, 145.9 (d, J = 252 Hz), 142.2 (d, J = 252 Hz), 141.5, 137.6 (d, J = 252 Hz), 134.0, 133.1, 131.2, 128.0, 109.1, 94.2, 54.2.

3: Obtained as a colorless oil in 90% yield. ^{1}H NMR (300 MHz, $CDCl_3$): δ 7.99 (d, 1H) 7.82 (d, 1H) 7.49-7.34 (m, 6H), 7.13 (t, 1H), 5.38 (s, 2H) in agreement with the literature.[36]

Compounds **2** and **4** were prepared by modifying a previously reported procedure and executed in air-free conditions.[36] 40 mL of degassed 4:1 THF:NEt_3 (v/v) were added to a round-bottom flask containing compound **1** or **3** (1 eq., 3.0 mmol), bis(triphenylphosphine)palladium(II) dichloride (0.05 equiv, 0.15 mmol) and copper (I) iodide (0.05 equiv, 0.15 mmol) under argon. Trimethylsilylacetylene (TMSA, 1.1 equiv, 3.3 mmol) was then added, and the reaction stirred for 16 hours at room temperature. Solvents were removed *in vacuo* and the crude product was purified by flash column chromatography on silica gel, using 2:1 CH_2Cl_2:hexanes as eluent and carried onto TMS deprotection

TMS-alkyne derived from 1: Obtained as an orange solid in 86% yield. ^{1}H NMR (500 MHz, $CDCl_3$): δ 7.89 (d, 1H), 7.61 (d, 1H), 7.48 (t, 1H), 7.37 (t, 1H), 5.47 (s, 2H), 0.28 (s, 9H). ^{13}C NMR (125 MHz, $CDCl_3$): δ 165.3, 145.7 (d, J = 252 Hz), 142.0 (d, J = 252 Hz), 137.4 (d, J = 252 Hz) 134.9, 131.9, 131.1, 130.4, 128.2, 123.7, 102.9, 100.5, 53.8, -0.3.

TMS-alkyne derived from 3: Obtained as an orange oil in 85% yield. ^{1}H NMR (300 MHz, $CDCl_3$): δ 7.92 (d, 1H) 7.59 (d,

1H), 7.46-7.35 (m, 7H), 5.39 (s, 2H), 0.23 (s, 9H) in agreement with the literature.[36]

Each TMS-alkyne (1 equiv, 2.0 mmol) was dissolved in 10 mL THF and cooled in an ice-water bath. Tetrabutylammonium fluoride (TBAF, 1.1 equiv, 2.2 mmol) was added as a 1.0 M solution in THF, and the reaction was stirred for ten minutes. The reaction mixture was then poured into water, and the product was extracted with diethyl ether, dried over $MgSO_4$, filtered, and concentrated *in vacuo* to yield a black residue. The crude product was purified by flash column chromatography on silica gel using 1:1 CH_2Cl_2:hexanes as eluent.

2: Obtained as a pink solid in 61% yield. ^{1}H NMR (300 MHz, $CDCl_3$): δ 7.90 (d, 1H), 7.62 (d, 1H), 7.49 (t, 1H) 7.39 (t, 1H), 5.45 (s, 2H) 3.35 (s, 1H). ^{13}C NMR (125 MHz, $CDCl_3$): δ 165.1, 145.0 (d, J = 252 Hz), 141.8 (d, J = 252 Hz), 137.5 (d, J = 252 Hz), 135.1, 132.2, 131.4, 130.5, 128.5, 122.9, 109.4, 82.6, 81.6, 53.9.

4: Obtained as a light pink oil in 62% yield. ^{1}H NMR (300 MHz, $CDCl_3$): δ 7.97 (d, 1H), 7.62 (d, 1H), 7.48-7.31 (m, 7H), 5.38 (s, 2H) 3.35 (s, 1H) in agreement with the literature.[36]

4,4'-Diiodotolane (Dihalide intermediate for **4-PE** compounds):

4,4'-Diaminotolane: According to a modified reported procedure,[10] executed under air- and water-free conditions, a 4:1 (v/v) THF:trimethylamine mixture (5 mL) was sparged with argon and added to a round bottom flask containing 4-ethynylaniline (1 equiv, 1.28 mmol), 4-iodoaniline (1 equiv, 1.28 mmol), bis(triphenylphosphine)palladium(II) dichloride (.05 equiv, .064 mmol) and copper (I) iodide (.05 equiv, .064 mmol). The resulting dark mixture was stirred overnight at room temperature under argon, while wrapped in aluminum foil. The reaction mixture was then poured into 10 mL of deionized water and extracted with CH_2Cl_2 (3x25mL). The combined organic layers were dried over magnesium sulfate, filtered, and concentrated *in vacuo* to yield a dark oily solid. Crude product was purified by flash column chromatography on silica, using 2% NEt_3 in CH_2Cl_2 to 5% NEt_3 in CH_2Cl_2 as eluent to yield 4,4'-diaminotolane as an orange solid in 56% yield. ^{1}H NMR (300 MHz, acetone-d6): δ 7.39 (d, 4H), 6.45 (d, 4H), 3.66 (bs, 4H), consistent with literature.[10]

4,4'-diiodotolane: Following a modified version of a previously reported procedure,[37] 4,4'-diaminotolane (1 equiv, 0.72 mmol) was suspended in 2.5 mL of 20% aqueous H_2SO_4 and cooled in an ice bath. A solution of $NaNO_2$ (2.25 equiv, 1.62 mmol) in 1 mL of H_2O was added to the suspension. After 30 minutes, compound **5** had dissolved to yield an orange solution. This solution was then added in portions to a solution of KI (10.5 equiv, 7.58 mmol) in 2 mL of H_2O. More H_2O was added to promote stirring, and the mixture stirred for 2 hours. The mixture was filtered, and the precipitate was washed with H_2O, and then with dilute aqueous sodium thiosulfate solution to yield **6** as a light brown solid in 45% yield. ^{1}H NMR (500 MHz, $CDCl_3$): δ 7.71 (d, 4H), 7.28 (d, 4H), consistent with a previous report.[37]

4,4'-Diiodo-2,2',6,6'-tetramethylbiphenyl (Dihalide intermediate for **4-TMBP-F5**) was prepared according to a previously reported procedure as follows:[38]

1,2-bis(3,5-dimethylphenyl)hydrazine: A suspension of 1,3-dimethyl-5-nitrobenzene (1 equiv, 13.2 mmol), zinc powder (5.8 equiv, 77 mmol), and EtOH (8 mL) was heated to reflux over 30 minutes. A solution of sodium hydroxide (5.7 equiv, 75 mmol) in water (10 mL) was added dropwise to the zinc suspension, resulting in an orange solution with suspended zinc. Heating was continued at reflux overnight, while more zinc powder (2.0 g) was added in portions over the first 4 hours. The hot suspension was then filtered over a bed of Celite into a solution of sodium bisulfite (200 mg) in 30% aqueous acetic acid (30 mL), and the filter cake rinsed with hot EtOH. The slurry was cooled in an ice bath and filtered, yielding an orange solid, which was recrystallized from heptane to yield the desired product as pale orange needles. ^{1}H NMR (500 MHz, $CDCl_3$): δ 6.52 (s, 6H), 5.50 (s, 2H), 2.27 (s, 12H), consistent a previous report[38] in 75% yield.

4,4'-Diamino-2,2',6,6'-tetramethylbiphenyl: 1,2-bis(3,5-dimethylphenyl)hydrazine (1 equiv, 3.32 mmol) was added to 10% HCl (40 mL), and the reaction mixture was heated at reflux. After 2 hours, all of the starting material had dissolved, and ^{1}H NMR showed consumption of the starting material. The reaction mixture was cooled to room temperature and the pH raised to > 10 with 1 M NaOH. The product was extracted using diethyl ether, washed with water and brine, dried over $MgSO_4$, filtered, and concentrated *in vacuo* to a red/orange oil, which solidified upon storage, to yield the desired product in 93% yield. This material was used without further purification. ^{1}H NMR (300 MHz, $CDCl_3$): δ 6.47 (s, 4H), 3.52 (s, 4H), 1.81 (s, 12H), consistent with a previous report.[38]

4,4'-Diiodo-2,2',6,6'-tetramethylbiphenyl): A solution of $NaNO_2$ (2.2 equiv, 4.35 mmol) in water (2 mL) was added to a suspension of 4,4'-Diamino-2,2',6,6'-tetramethylbiphenyl (1 equiv, 1.94 mmol) and 33% aqueous H_2SO_4 (12 mL) in an ice bath. After approximately 30 min, the starting material had dissolved, and the reaction mixture was transferred to a solution of I_2 (2.8 equiv, 5.32 mmol) and NaI (4.7 equiv, 9 mmol) in water (2.5 mL) at 0°C. 10 mL of water and 25 mL of CH_2Cl_2 were added, and the reaction mixture stirred overnight at room temperature. Sodium thiosulfate (1 g) was added and the reaction mixture stirred for additional 30 minutes. The mixture was filtered, resulting in a two-phase filtrate that was separated. The aqueous phase was extracted with chloroform, and the combined organic phases were washed with 10% aqueous sodium thiosulfate solution and brine, dried over $MgSO_4$, filtered, and concentrated *in vacuo* to yield a dark yellow solid. Crude product was purified by flash column chromatography on silica, using hexanes as eluent, to yield the desired product as colorless solid in 42% yield. ^{1}H NMR (300 MHz, $CDCl_3$): δ 7.48 (s, 4H), 1.83 (s, 12H), consistent with a previous report.[38]

General Procedure for Sonogashira Reactions: The reaction solvent of 5:1 THF:NEt_3 (v/v) or 1:1 THF:NEt_3 was deoxygenated by sparging with argon for 20 minutes, and

added to a round bottom flask containing **2** or **4** (2.1 equiv), diiodide core (1 equiv), copper (I) iodide (.05 equiv), and bis(triphenylphosphine)palladium(II) dichloride (.05 equiv) under argon, and stirred overnight. The reaction was monitored by TLC, and completion was judged based on consumption of the diiodide. Solvents were then removed *in vacuo*, and the resulting crude product was purified by flash column chromatography and recrystallization, details of which are described for each target compound below.

4-BP-F5: Prepared according to the general Sonogashira procedure, using 1.53 mmol of **2**, 0.70 mmol of 4,4'-diiodobiphenyl, 0.035 mmol $Cl_2Pd(PPh_3)_2$, 0.035 mmol of CuI, and 30 mL of 5:1 THF:NEt_3. 1:1 CH_2Cl_2:hexanes was used as chromatography eluent, and the product was recrystallized from hexanes in 44% yield. ^{1}H NMR (500 MHz, $CDCl_3$): δ 8.04 (d, 2H) 7.68 (d, 2H), 7.62 (d, 2H), 7.58-7.53 (m, 6H), 7.44 (t, 2H), 5.50 (s, 4H). ^{13}C NMR (125 MHz, $CDCl_3$): δ 165.5, 145.7 (d, J = 252 Hz), 141.5 (d, J = 252 Hz), 140.5, 137.5 (d, J = 252 Hz), 134.2, 132.3, 131.8, 131.0, 130.6, 128.1, 126.9, 124.0, 122.3, 109.3, 94.3, 88.8, 53.9.

4-BT-F5: Prepared according to general Sonogashira procedure, using 0.82 mmol of **2**, 0.41 mmol 4,4'-diiodobithiophene, 0.02 mmol $Cl_2Pd(PPh_3)_2$, 0.02 mmol of CuI, and 24 mL of 5:1 THF:NEt_3. 1:1 CH_2Cl_2:hexanes was used as chromatography eluent. **4-BT-F5** was recrystallized from acetone/water in 63% yield. ^{1}H NMR (500 MHz, $CDCl_3$): δ 8.03 (d, 2H), 7.65 (d, 2H), 7.54 (t, 2H), 7.43 (t, 2H), 7.17 (d, 2H), 7.13 (d, 2H). ^{13}C NMR (125 MHz, $CDCl_3$): δ 165.2, 145.8 (d, J = 252 Hz), 141.8 (d, J = 252 Hz), 137.5 (d, J = 252 Hz), 138.6, 134.0, 133.1, 132.3, 131.0, 130.3, 128.3, 124.1, 123.5, 122.4, 109.3, 93.2, 87.7, 54.0.

4-DMF-F5: Prepared according to general Sonogashira procedure, using 0.26 mmol of **2**, 0.13 mmol of 2,7-diiodo-9,9-dimethylfluorene, 0.007 mmol of $Cl_2Pd(PPh_3)_2$, 0.007 mmol of CuI, and 12 mL of 5:1 THF:NEt_3. 1:1 CH_2Cl_2:hexanes was used as chromatography eluent, and **4-DMF-F5** was then recrystallized from acetone/water in 75% yield. ^{1}H NMR (500 MHz, $CDCl_3$): δ 8.02 (d, 2H), 7.74-7.69 (m, 4H), 7.63 (s, 2H), 7.56 (t, 2H), 7.49-7.41 (m, 4H), 5.52 (s, 4H), 1.57 (s, 6H). ^{13}C NMR (125 MHz, $CDCl_3$): δ 165.4, 154.1, 145.7 (d, J = 252 Hz), 141.7 (d, J = 252 Hz), 139.0, 137.5, 134.2, 132.3, 130.84, 130.8, 130.5, 128.0, 125.8, 124.2, 122.0, 120.2, 109.4, 95.5, 88.3, 53.9, 47.0, 26.8.

4-TMBP-F5: Prepared according to general Sonogashira procedure, using 0.11 mmol of compound **9**, 0.24 mmol of **2**, 0.01 mmol of $Cl_2Pd(PPh_3)_2$, 0.01 mmol of CuI, and 6 mL of 5:1 THF:NEt_3. 1:1 CH_2Cl_2:hexanes was used as chromatography eluent, and **4-TMBP-F5** was recrystallized from acetone/water in 43% yield. ^{1}H NMR (500 MHz, $CDCl_3$): δ 7.99 (d, 2H), 7.65 (d, 2H), 7.51 (t, 2H), 7.38 (t, 2H), 7.27 (s, 4H), 5.49 (s, 4H), 1.91 (s, 12H). ^{13}C NMR (125 MHz, $CDCl_3$): δ 165.5, 145.8 (d, J = 252 Hz), 141.8 (d, J = 252 Hz), 140.3, 137.5 (d, J = 252 Hz), 135.8, 134.4, 132.2, 130.8, 130.63, 130.4, 127.8, 124.3, 121.6, 109.5, 95.1, 87.3, 54.0, 19.5.

3-DBPE-F5: Prepared according to general Sonogashira procedure, using 0.23 mmol of compound **2,** 0.11 mmol of 1,4-dibutoxy-2,5-diiodobenzene, 0.006 mmol of $Cl_2Pd(PPh_3)_2$, 0.006 mmol of CuI, and 10 mL of 1:1 THF:NEt_3. 1:1 CH_2Cl_2:hexanes was used as chromatography eluent, and **3-DBPE-F5** was recrystallized from chloroform/methanol in 54% yield. ^{1}H NMR (500 MHz, $CDCl_3$): δ 8.00 (d, 2H), 7.69 (d, 2H), 7.55 (t, 2H), 7.41 (t, 2H), 7.02 (s, 2H), 4.05 (t, 4H), 1.87 (quin, 4H), 1.57 (sext, 4H) 1.00 (t, 6H). ^{13}C NMR (125 MHz, $CDCl_3$): δ 165.2, 153.7, 145.7 (d, J = 252 Hz), 141.7 (d, J = 252 Hz), 137.5 (d, J = 252 Hz), 134.4, 132.2, 130.7, 130.3, 127.9, 124.5, 116.9, 114.2, 109.4, 93.2, 91.5, 69.4, 53.8, 31.4, 19.2, 13.9.

4-PE-F5: Prepared according to general Sonogashira procedure, using 0.26 mmol of **2**, 0.13 mmol of compound **6**, 0.007 mmol $Cl_2Pd(PPh_3)_2$, 0.007 mmol of CuI, and 12 mL of 5:1 THF:NEt_3. 1:1 CH_2Cl_2:hexanes used as chromatography eluent, and **4-PE-F5** was recrystallized from acetone/water in 75% yield. ^{1}H NMR (500 MHz, $CDCl_3$): δ 8.02 (d, 2H), 7.67 (d, 2H), 7.58-7.41 (m, 12H), 5.50 (s, 4H). ^{13}C NMR (125 MHz, $CDCl_3$): δ 165.3, 145.9 (d, J = 252 Hz), 141.8 (d, J = 252 Hz), 137.5 (d, J = 252 Hz), 134.2, 132.3, 131.5, 131.4, 130.9, 130.6, 128.2, 123.8, 123.3, 123.1, 109.3, 94.2, 91.0, 89.8, 54.0.

4-PE-H5: Prepared according to general Sonogashira procedure, using 0.55 mmol of **4**, 0.25 mmol compound **6**, 0.013 mmol $Cl_2Pd(PPh_3)_2$, 0.013 mmol of CuI, and 12 mL of 5:1 THF:NEt_3. 1:1 CH_2Cl_2:hexanes was used as chromatography eluent, and **4-PE-H5** was recrystallized from acetone/water in 22% yield. ^{1}H NMR (500 MHz, $CDCl_3$): δ 8.06 (d, 2H) 7.68 (d, 2H) 7.56-7.49 (m, 10H) 7.44-7.36 (m, 12H), 5.45 (s, 4H). ^{13}C NMR (125 MHz, $CDCl_3$): δ 166.1, 135.8, 134.2, 131.9, 131.7, 131.5, 130.8, 128.6, 128.4, 128.3, 128.2, 123.6, 123.3, 123.0, 94.1, 91.1, 90.3, 67.2.

3-PE-F5: Prepared according to general Sonogashira procedure, using 0.48 mmol of **2**, 0.24 mmol of 1,4-diiodobenzene, 0.012 mmol $Cl_2Pd(PPh_3)_2$, 0.012 mmol of CuI, and 12 mL of 5:1 THF:NEt_3. 1:1 CH_2Cl_2:hexanes was used as chromatography eluent, and **3-PE-H5** was recrystallized from acetone in 61% yield. ^{1}H NMR (500 MHz, $CDCl_3$): δ 8.02 (d, 2H), 7.69 (d, 2H), 7.56 (t, 2H), 7.48 (s, 4H) 7.43 (t, 2H), 5.5 (s, 4H). ^{13}C NMR (125 MHz, $CDCl_3$): δ 165.3, 145.8 (d, J = 252 Hz), 141.8 (d, J = 252 Hz), 137.5 (d, J = 252 Hz), 134.3, 132.3 131.4, 130.9, 130.6, 128.2, 123.8, 123.3, 109.4, 94.2, 89.8, 53.9.

3-PE-H5: Prepared according to general Sonogashira procedure, using 0.67 mmol of **4**, 0.33 mmol of 1,4-diiodobenzene, 0.02 mmol $Cl_2Pd(PPh_3)_2$, 0.02 mmol of CuI, and 12 mL of 5:1 THF:NEt_3. 3:1 CH_2Cl_2:hexanes was used as chromatography eluent, and **3-PE-H5** was recrystallized from acetone/water in 70% yield. ^{1}H NMR (500 MHz, $CDCl_3$): δ 8.02 (d, 2H), 7.65 (d, 2H), 7.53-7.28 (m, 18H). ^{13}C NMR (75 MHz, $CDCl_3$): δ 166.1, 135.8, 134.2, 131.9, 131.7, 131.6, 130.8, 128.6, 128.4, 128.3, 128.2, 123.6, 123.2, 94.2, 90.2, 67.1.

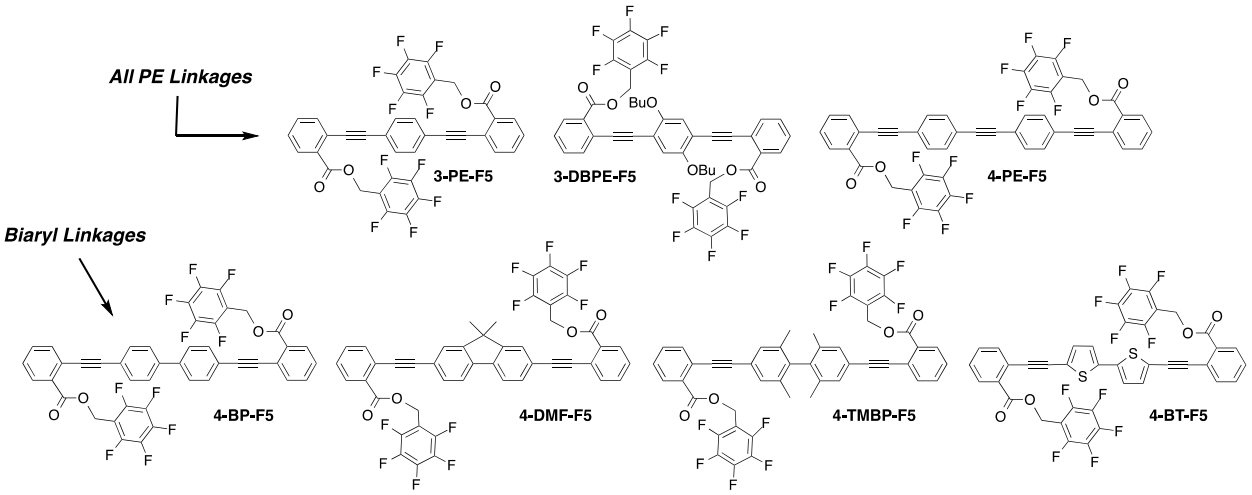

Figure 2. Seven pentafluorobenzyl benzoate-substituted PEs studied in this work.

Results and Discussion

Molecular Design and Synthesis

In contrast to our previous three-ring PEs that twist in response to ArF-ArH interactions of a central terephthalate with fluorinated benzyl esters, molecules presented here comprise pentafluorobenzyl *o*-ethynylbenzoate esters attached to both termini of a conjugated core (Figure 1). With the hypothesis that intramolecular ArF-ArH stacking would twist the PE linkages, we prepared and determined crystal structures for seven such molecules, which had either three or four conjugated arenes as the "main chains" of the chromophores (Figure 2). Scheme 1 shows how we prepared *o*-ethynyl benzyl benzoates **2** (perfluorobenzyl) and **4** (benzyl): esterification of 2-iodobenzoic acid with perfluorobenzyl alcohol or benzyl alcohol yielded pentafluorobenzyl esters **1** and **3**, followed by Sonogashira cross-coupling with trimethylsilylacetylene and subsequent deprotection of the trimethylsilyl group with tetrabutylammonium fluoride yielded the common ethynyl intermediates **2** and **4**. Sonogashira reactions between these alkynes and various dihalides, which were either commercially available or prepared according to literature procedures, provided the target compounds shown in Figure 2. We grew X-ray quality single crystals for each of these molecules.

Scheme 1. Synthesis of ethynyl intermediates **2** and **4** and representative couplings to prepare conjugated molecules with potential for intramolecular aromatic interactions.

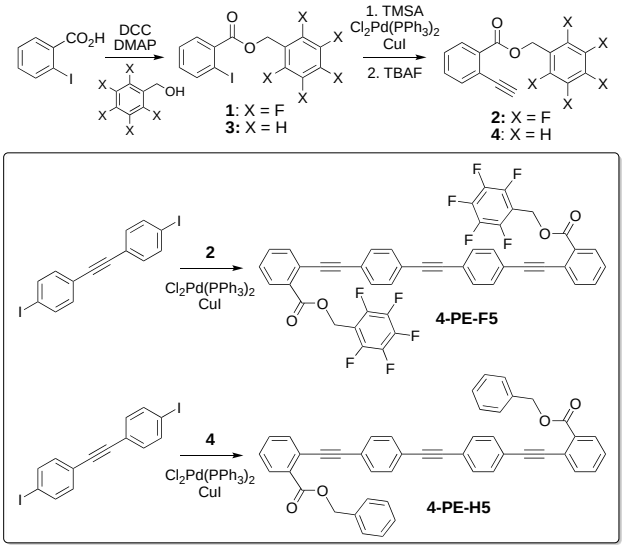

X-Ray Crystallography

Molecules with only PE linkages

We first sought to establish the viability of our design in Figure 1 for broadening the applicability of this approach to controlling solid conjugated materials. We hypothesized that the same key components in this different configuration would, within three-ring and four-ring PEs: i) participate in intramolecular ArF-ArH stacking interactions and ii) induce twisting of PEs with such stacking interactions. As described below, the crystal structures of PEs described here strongly support potential generality of this design by showing intramolecular cofacial ArF-ArH stacking, with each instance of this stacking yielding a twisted PE linkage.

The simplest molecule we investigated is **3-PE-F5**, which comprises an unsubstituted central PE ring flanked on each

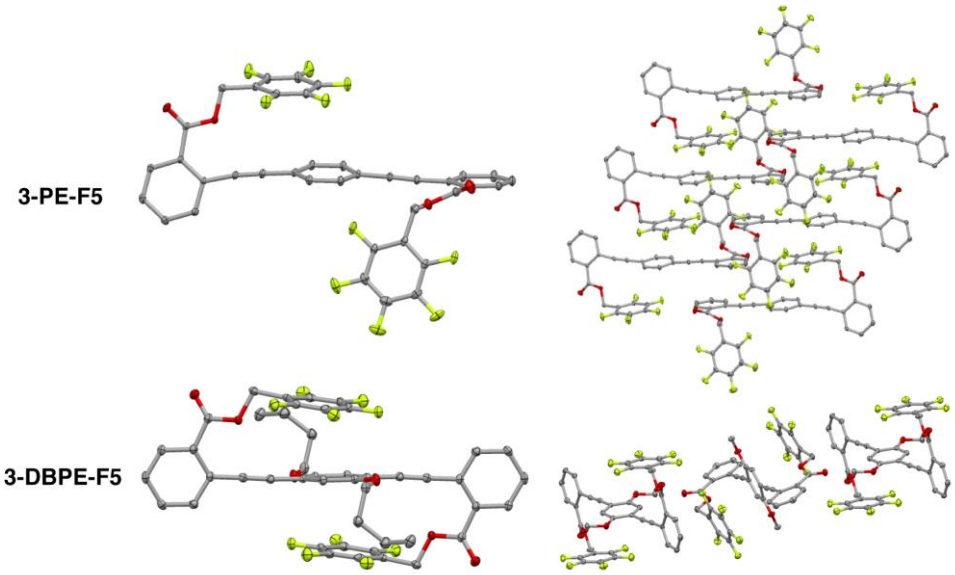

Figure 3. X-ray crystal structures of **3-PE-F5** (top) and **3-DiOR-PE-F5** (bottom). Hydrogen atoms and outer three carbon atoms of the butoxy chains of **3-DiOR-PE-F5** are omitted for clarity. Thermal ellipsoids shown at 50% probability.

side by pentafluorobenzyl benzoates. The crystal structure shows that only one of these two ArF rings participates in both intramolecular and intermolecular ArF-ArH slipped-stacks with central PE rings, each with closest contacts between carbon atoms < 3.4 Å. These stacking interactions form infinite slipped columns along the crystallographic *a*-axis, along which infinite slip-stacked interactions between benzoate rings also extend. Importantly, the PE linkage across which the ArF-ArH cofacial interactions occur is twisted, with torsional angles of 67°, while the other PE linkage is coplanar (< 10° torsions); instead of intramolecular stacking interactions, the two faces of this ArF ring: i) stack with benzoate rings of another molecule, and ii) interact with the edge of an ArF ring of another molecule.

An analogous PE is **3-DBPE-F5**, which has two *n*-butoxy substituents on the central ring. Intramolecular cofacial ArF-ArH interactions of similar configuration figure prominently in this structure, with each face of the electron-rich dialkoxy ring stacking with one of the ArF rings, with closest C•••C contacts of 3.47 Å between the rings (Figure 3). The opposite, outward-pointing face of each of the ArF rings stack with a benzoate ring of another PE. This overall pattern is distinct from the unsubstituted central ring in **3-PE-F5**, which only shows stacking on one face of the central ring. We attribute this difference to the electron-donating capability of the alkoxy substituents on the central ring making the ArF-ArH interactions more favorable. As in other examples, this stacking through the benzylic ester linkers twists the PE linkages, in this case along both alkynes, with torsional angles between 85-90°.

Having established the viability of the pentafluorobenzyl *o*-ethynylbenzoate unit as capable of introducing twisting in two different three-ring PEs, we integrated it into the termini of a four-ring PE—**4-PE-F5—**to test the hypothesis that this moiety

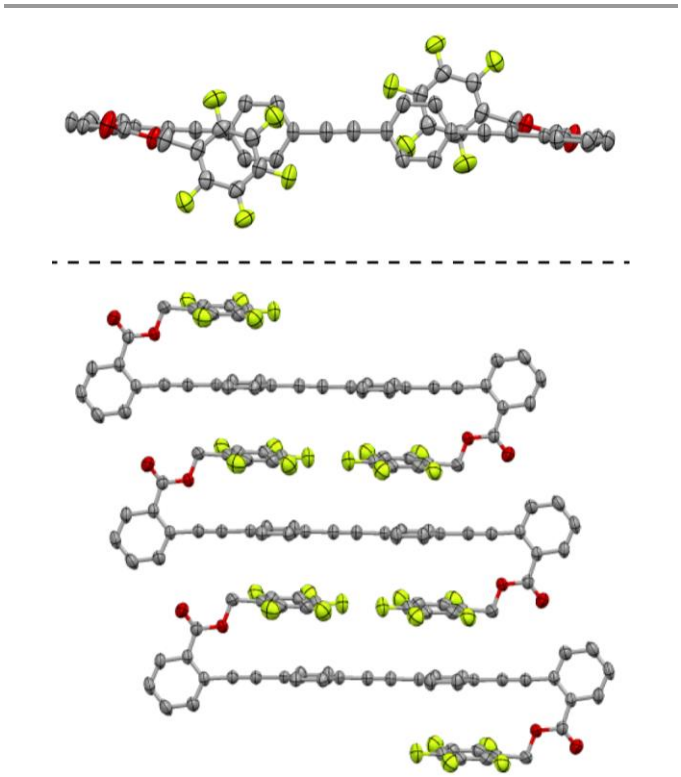

Figure 4. X-ray crystal structure of an individual molecule (top) and three molecules connected through intramolecular ArF-ArH stacking interactions of **4-PE-F5**. Thermal ellipsoids shown at 50% probability. Hydrogen atoms omitted for clarity.

can twist PE linkages in longer molecules. The crystal structure reveals that each of the two ArF rings stack intramolecularly with ArH rings in the middle of the main chain, with closest C•••C distances of 3.59 Å. The second of the three PE linkages is coplanar, with inter-ring torsional angles of < 3°, and these two coplanar arenes stack intramolecularly with neighboring

ArF rings on opposite faces of the PE. As in the three-ring PEs, these intramolecular ArF-ArH interactions yield large torsions (78-82°) between the central and terminal PE rings

A characteristic that four-ring molecules share with our previously reported, terephthalate-based three-ring PEs is an equal number of fluorinated rings and potential stacking partners separated from the benzoate ring by alkynes. Such balancing of the "stoichiometry" of electron-rich and electron-poor arenes introduces the potential for stacks of alternating ArF and ArH rings, similar to that in the cocrystalline solid of hexafluorobenzene and benzene.[39] Among the five different four-ring chromophores we studied, only **4-PE-F5** displayed this feature, with infinite ArF-ArH stacks that propagate along the crystallographic *b* axis. The intermolecular ArF-ArH interactions hold the rings with closest C•••C distances < 3.5 Å and centroid-to-centroid distance of 3.72 Å, as opposed to 4.18 Å for the intramolecular pairs (Figure 4).

We also crystallized two analogous compounds that have non-fluorinated benzyl pendants instead of the pentafluorinated rings (Figure 5). The three-ring PE analog **3-PE-H5** has a crystal structure similar to that of **3-PE-F5**, in that one pendant ring interacts cofacially with the central ring, while one does not. Key differences, however, are that the cofacial rings are further apart in this structure (3.7 Å) than in **3-PE-F5**, and that one of the pendant benzyl groups participates in edge-face interactions with the central ring. More strikingly different is the comparison of **4-PE-F5** to its non-fluorinated analog, **4-PE-H5**. Instead of cofacial stacking of pendant and main-chain rings, pendant rings of **4-PE-H5** undergo edge-face interactions with the central PE rings, allowing PE backbones to interact with each other intermolecularly through edge-face interactions.

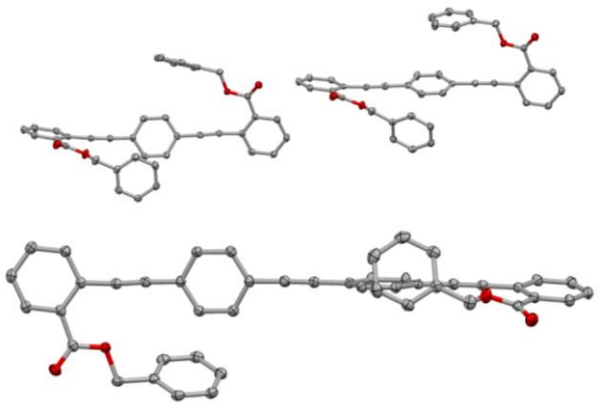

Figure 5. X-ray crystal structures of **3-PE-H5** (top) and **4-PE-H5**, each featuring prominent edge-face interactions. Thermal ellipsoids shown at 50% probability. A disordered $CHCl_3$ molecule from the structure of **4-PE-H5** is omitted for clarity, as are hydrogen atoms from both structures.

Molecules With Central Biaryl Linkages

To probe the applicability of this approach to molecules with greater diversity of linkages, we crystallized four molecules that each have single bonds between two central arenes. As expected based on inter-ring steric interactions, a biphenyl linkage yields non-planar torsional angles of 18° in **4-BP-F5**, with disorder about the inversion center. Although disordered $CHCl_3$ molecules in this particular structure appear to preclude intermolecular stacking of the ArF rings, intramolecular ArF-ArH stacking between the terminal and central rings of the conjugated main chain twists the PE linkages out of planarity by 77-85°. The ArF ring bends closer to the main chain than in other examples, with C•••C distances as close as 3.17 Å.

With the hypothesis that it would result in twisting between each ring along the conjugated backbone, we prepared and crystallized **4-TMBP-F5**. Steric interactions between *ortho*-methyl groups force the central two rings of the biphenyl moiety to be nearly orthogonal, which therefore presents ArH faces that point along different directions for intramolecular interactions with ArF pendants. Although these types of interactions do occur in the crystal structure, the interacting ArF and ArH rings are not fully coplanar and are further separated from each other than in the unmethylated biphenyl derivative, which we attribute to steric repulsion between the ArF rings and methyl groups. Nevertheless, the PE linkages of **4-TMBP-F5** are twisted, with torsional angles of 62-66° on one side, and 32-34° on the other (Figure 6).

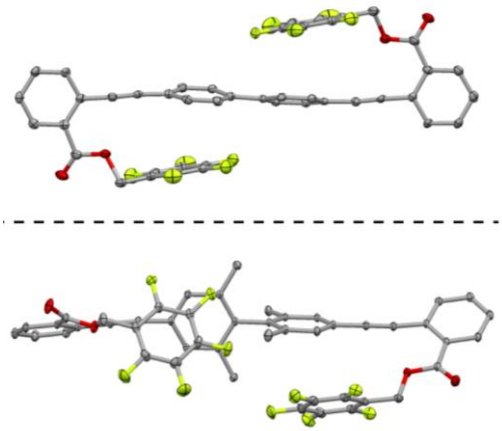

Figure 6. X-ray crystal structure of biphenyl-based four-ring PEs that show two intramolecular ArF-ArH stacking interactions: **4-BP-F5** (top), **4-TMBP-F5** (bottom). Thermal ellipsoids shown at 50% probability. Hydrogen atoms omitted for clarity.

Two related molecules had highly coplanar biaryl central linkages in the crystal structures. In one example, a 9,9-dimethylfluorene unit enforced coplanar central rings. Intramolecular ArF-ArH interactions occur on only one of the two termini—as seen in **3-PE-F5**, the PE linkage across which the stacking interaction occurs is twisted, with an 89° torsional angle, while the other side of the 4-ring main chain, which lacks the ArF-ArH stacking, has a torsional angle < 20° (Figure 7). The ArF rings of this molecule also participate in other, intermolecular cofacial stacking interactions with benzoate

Table 1. UV/vis and fluorescence parameters of all molecules investigated in both dilute CH_2Cl_2 solution and as solution-cast thin films.

Compound	Solution			Thin Film		
	λ_{max}(abs)	λ_{max}(emis)	Φ_F	λ_{max}(abs)	λ_{max}(emis)	Emission Shift
3-PE-F5	339 nm	379 nm	0.64	339 nm	406 nm	27 nm
3-PE-H5	338 nm	377 nm	0.76	343 nm	415 nm	38 nm
3-DBPE-F5	378 nm	441 nm	0.71	381 nm	439 nm	-2 nm
4-PE-F5	346 nm	392 nm	0.75	353 nm	403 nm	11 nm
4-PE-H5	348 nm	390 nm	0.94	355 nm	425 nm	35 nm
4-BP-F5	339 nm	391 nm	0.69	335 nm	422 nm	31 nm
4-TMBP-F5	323 nm	377 nm	0.08	324 nm	386 nm	9 nm
4-DMF-F5	361 nm	402 nm	0.77	356 nm	433 nm	31 nm
4-BT-F5	398 nm	461 nm	0.24	396 nm	517 nm	56 nm

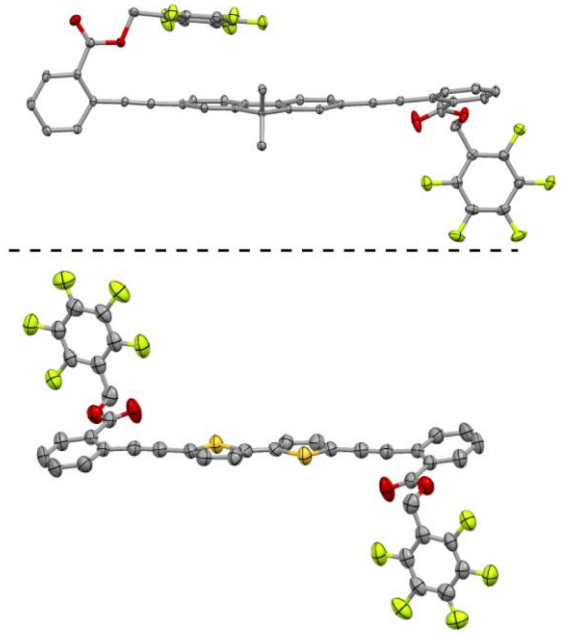

Figure 7. X-ray crystal structure of four-ring PEs that show one or zero intramolecular ArF-ArH interactions: **4-DMF-F5** (top) and **4-BT-F5** (bottom). Thermal ellipsoids shown at 50% probability. Hydrogen atoms omitted for clarity.

rings. Potential explanations for only one intramolecular ArF-ArH interaction occurring include increased steric interactions between the ArF ring and the methyl groups of the fluorene unit, or as we surmised based on the substituent effects in the 3-ring PEs, a decrease in electrostatic driving force for a second co-facial interaction of the highly coupled arene rings within the fluorene, relative to the observed intramolecular cofacial interactions. Finally, the bithiophene-core derivative **4-BT-F5** lacks any ArF-ArH interactions, which we found somewhat surprising, as ArF-thiophene cofacial stacking interactions have precedent in small conjugated molecules.[40-42] Inter-ring torsions both across each of the alkynes and across the 2,2'-bithiophene unit are less than 20°. Apparently, the energy of interaction between the thiophene and perfluorinated rings is not competitive in this arrangement, an observation that we are currently investigating. Potential explanations are reduced London dispersion forces between the ArF ring and the smaller thiophene rings as compared to ArF-phenyl interactions, or the larger π-orbitals on the sulfur atoms of thiophene rings.

Optical Spectroscopy

UV/vis absorbance and fluorescence emission spectra of all compounds were obtained both as dilute solutions in CH_2Cl_2, as well as solution-cast thin films. In solution, structure-property relationships were consistent with well-established trends in conjugated materials. For example, the spectra of **3-PE-F5** were hypsochromically shifted from the longer yet similarly substituted phenylene-ethynylene **4-PE-F5**. Whether the benzyl pendants were substituted with five fluorine atoms or five hydrogen atoms had virtually no impact on the shape or position of spectra ($\Delta\lambda_{max} \leq 2$ nm) for either **3-PE-F5/H5** or **4-PE-F5/H5**. For the three compounds that have biphenyl linkages between the central rings, the trend of spectral position correlates with expected (and crystallographically observed) dihedral angles of the biphenyl units, with the most twisted linkage of **4-TMBP-F5** yielding the most hypsochromically shifted spectra, while the coplanar fluorene linkage is 30-40 nm red-shifted from the tetramethylbiphenyl derivative. The bithiophene derivative has the lowest energy optical spectra of the compounds investigated here—the more electron rich nature of thiophene rings typically yields bathochromically shifted spectra when compared to phenyl analogs.[43]

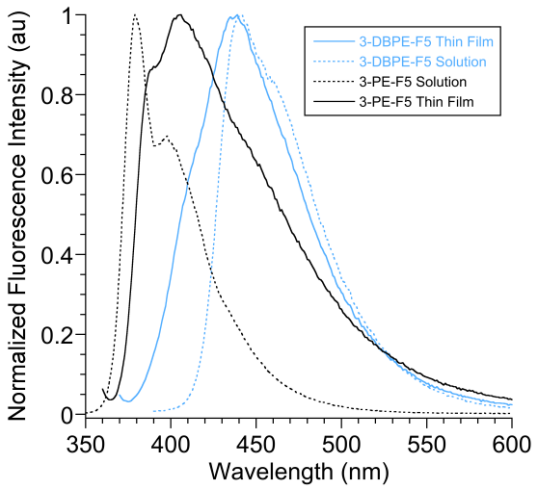

Figure 8. Height-normalized emission spectra of **3-DBPE-F5** (blue curves) and **3-PE-F5** (black curves) either dissolved in CH_2Cl_2 (dotted lines) or as drop-cast thin films (solid lines), highlighting the bathochromic shift of **3-PE-F5** that is absent in **3-DBPE-F5**.

In all compounds, there exist only small differences between the spectra of solids and solutions of these compounds. However, the differences in solid-state packing observed in crystal structures lead to important distinctions in the emission spectroscopy of solution-cast thin films of these compounds. Similarly, there is correlation between the crystal structures and optical properties of the three-ring PEs. The solid-state emission spectrum of **3-DBPE-F5**, the crystal structure of which shows a fully twisted PE backbone, has almost no shift relative to solution; in contrast, **3-PE-F5** and **3-PE-H5**, the crystal structures of which each show one coplanar linkage along the PE backbones and extensive interactions between the PE chromophore moieties, show 27-38 nm bathochromic shifting when comparing solid to solution emission spectra (Figure 8).

In examining the four-ring compounds, the most obvious impact of packing comes from simple visual inspection of luminescence (see TOC image), which indicates that **4-PE-F5** is obviously more fluorescent than **4-PE-H5.** We estimated the relative quantum yields of fluorescence of thin films of these two compounds by comparing their fluorescence intensities at indistinguishable absorbance values under otherwise identical experimental conditions (see ESI). This experiment indicated that **4-PE-F5** 5-7x more fluorescent than the hydrogenated analog (Figure 9). In addition, the weak emission of **4-PE-H5** is bathochromically shifted over 20 nm relative to the spectrum of **4-PE-F5**, which has a sharp band with maximum at 403 nm. We attribute these observations to the ArF-ArH cofacial interactions of **4-PE-F5** preventing aggregation and coupling between chromophores that could otherwise yield aggregation-caused quenching. Finally, in comparing the solution-state and solid-state spectra of the four biaryl-linked compounds, the least shifted of the emission spectra is highly twisted in the solid state (**4-TMBP-F5**). On the other hand, the most shifted of the solid-state emission spectra relative to solution is **4-BT-F5**, which we attribute to a combination of interchromophore interactions and coplanarity of the backbone observed in the crystal structure.

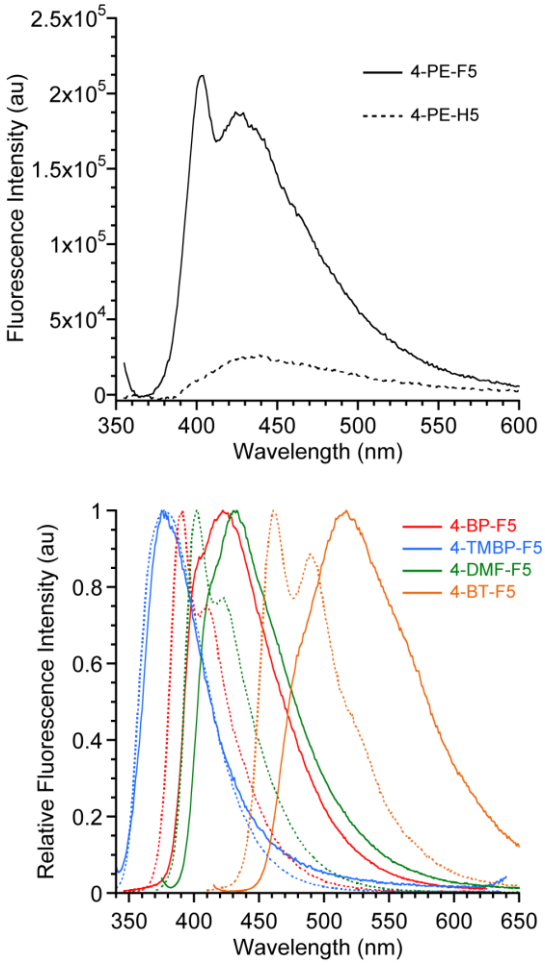

Figure 9. Fluorescence emission spectra demonstrating select comparisons. *Top:* Fluorescence emission spectra of thin films of fluorinated and non-fluorinated 4-ring phenylene-ethynylenes, highlighting protection from quenching of **4-PE-F5** by ArF-ArH interactions. The two films had indistinguishable absorbances (0.025) at λ_{ex} (345 nm). *Bottom:* Comparison of solution state (dotted lines) and thin films (solid lines) of the four biaryl-linked four-ring conjugated molecules.

Conclusion

In six of the seven fluorinated compounds described here, intramolecular ArF-ArH stacking interactions between pendant pentafluorobenzyl rings and arenes in the conjugated backbone occur. Moreover, *each* example of intramolecular ArF-ArH stacking yields twisting about the ethynyl linkages across which the stacking occurs, including in molecules with four conjugated rings. In the absence of such interactions, however, the conformations of the arylethynyl linkages are unpredictable. ArF-ArH-induced twisting impacts optoelectronic properties of some of these solids, such as enhanced fluorescence quantum yields or reduced bathochromic shifts when compared to solution.

This work has several important implications for the rational design of conjugated materials. First, it demonstrates

the general utility of installing pentafluorobenzyl esters into conjugated materials to twist arylethynyl linkages in the solid state reliably. This work broadens ArF-ArH interactions as a supramolecular synthon to twist PEs both in terms of the length of the conjugated chromophore as well as the integration of non-alkynyl linkages. Second, it reinforces the potential for electronic substituent effects to increase the likelihood of observing these interactions and programmed twisting, as demonstrated here with the contrast of **3-PE-F5 and 3-DBPE-F5**. Third, conjugated materials that are twisted out of coplanarity have potential inhibition of self-quenching of luminescence, as demonstrated here with **4-PE-H5** and **4-PE-F5,** and responses to stimuli that increase planarity and intermolecular aggregation. Therefore, although challenges such as successful integration of heteroaromatic thiophene-based rings arise, this work demonstrates how discrete, directional aromatic interactions, particularly those involving non-conjugated pendants, can play critical roles in the rational design over the solid-state packing and properties of conjugated materials.

Conflicts of interest

There are no conflicts to declare.

Acknowledgements

This work was supported by the Department of Energy, Basic Energy Sciences, through award DE-SC0016423

Notes and references

1. O. Ostroverkhova, *Chem. Rev.*, 2016, **116**, 13279-13412.
2. E. Thanayupong, K. Suttisintong, M. Sukwattanasinitt and N. Niamnont, *New J. Chem.*, 2017, **41**, 4058-4064.
3. I. B. Kim, B. Erdogan, J. N. Wilson and U. H. F. Bunz, *Chem. Eur. J.*, 2004, **10**, 6247-6254.
4. H. Jiang, P. Taranekar, J. R. Reynolds and K. S. Schanze, *Angew. Chem. Int. Ed.*, 2009, **48**, 4300-4316.
5. Y. Tang, T. S. Corbitt, A. Parthasarathy, Z. Zhou, K. S. Schanze and D. G. Whitten, *Langmuir*, 2011, **27**, 4956-4962.
6. H. C. Pappas, S. Phan, S. Yoon, L. E. Edens, X. Meng, K. S. Schanze, D. G. Whitten and D. J. Keller, *ACS Appl. Mater. Interf.*, 2015, **7**, 27632-27638.
7. Y. Wang, K. S. Schanze, E. Y. Chi and D. G. Whitten, *Langmuir*, 2013, **29**, 10635-10647.
8. H. Masai, T. Fujihara, Y. Tsuji and J. Terao, *Chem. Eur. J.*, 2017, **23**, 15073-15079.
9. J.-T. Zheng, R.-W. Yan, J.-H. Tian, J.-Y. Liu, L.-Q. Pei, D.-Y. Wu, K. Dai, Y. Yang, S. Jin, W. Hong and Z.-Q. Tian, *Electrochim. Acta*, 2016, **200**, 268-275.
10. Q. Lu, K. Liu, H. Zhang, Z. Du, X. Wang and F. Wang, *ACS Nano*, 2009, **3**, 3861-3868.
11. J. K. Mwaura, M. R. Pinto, D. Witker, N. Ananthakrishnan, K. S. Schanze and J. R. Reynolds, *Langmuir*, 2005, **21**, 10119-10126.
12. G. Adam, T. Yohannes, M. White, A. Montaigne, C. Ulbricht, E. Birckner, S. Rathgeber, C. Kaestner, H. Hoppe, N. S. Sariciftci and D. A. M. Egbe, *Macromol. Chem. Phys.*, 2014, **215**, 1473-1484.
13. D. A. M. Egbe, S. Tuerk, S. Rathgeber, F. Kuehnlenz, R. Jadhav, A. Wild, E. Birckner, G. Adam, A. Pivrikas, V. Cimrova, G. Knoer, N. S. Sariciftci and H. Hoppe, *Macromolecules*, 2010, **43**, 1261-1269.
14. K. Okuyama, T. Hasegawa, M. Ito and N. Mikami, *J. Phys. Chem.*, 1984, **88**, 1711-1716.
15. J. M. Seminario, A. G. Zacarias and J. M. Tour, *J. Am. Chem. Soc.*, 1998, **120**, 3970-3974.
16. D. Yan and D. G. Evans, *Mater. Horizons*, 2014, **1**, 46-57.
17. S. Varghese and S. Das, *J. Phys. Chem. Lett.*, 2011, **2**, 863-873.
18. M. D. Curtis, J. Cao and J. W. Kampf, *J. Am. Chem. Soc.*, 2004, **126**, 4318-4328.
19. S. Menning, M. Kraemer, B. A. Coombs, F. Rominger, A. Beeby, A. Dreuw and U. H. F. Bunz, *J. Am. Chem. Soc.*, 2013, **135**, 2160-2163.
20. G. Brizius, K. Billingsley, M. D. Smith and U. H. F. Bunz, *Org. Lett.*, 2003, **5**, 3951-3954.
21. A. Beeby, K. S. Findlay, A. E. Goeta, L. Porres, S. R. Rutter and A. L. Thompson, *Photochem. Photobiol. Sci.*, 2007, **6**, 982-986.
22. J.-S. Yang, J.-L. Yan, C.-Y. Hwang, Y. Shih, Chiou, K.-L. Liau, H.-H. G. Tsai, G.-H. Lee and S.-M. Peng, *J. Am. Chem. Soc.*, 2006, **128**, 14109-14119.
23. C. Rest, R. Kandanelli and G. Fernandez, *Chem. Soc. Rev.*, 2015, **44**, 2543-2572.
24. A. Mukherjee, *Cryst. Growth Des.*, 2015, **15**, 3076-3085.
25. W. Hu, N. Zhu, W. Tang and D. Zhao, *Org. Lett.*, 2008, **10**, 2669-2672.
26. E. A. Meyer, R. K. Castellano and F. Diederich, *Angew. Chem. Int. Ed.*, 2003, **42**, 1210-1250.
27. J. W. Hwang, P. Li and K. D. Shimizu, *Org. Biomol. Chem.*, 2017, **15**, 1554-1564.
28. F. Ponzini, R. Zagha, K. Hardcastle and J. S. Siegel, *Angew. Chem. Int. Ed.*, 2000, **39**, 2323-2325.
29. R. Xu, W. B. Schweizer and H. Frauenrath, *Chem. Eur. J.*, 2009, **15**, 9105-9116.
30. Y. Sakamoto, T. Suzuki, M. Kobayashi, Y. Gao, Y. Fukai, Y. Inoue, F. Sato and S. Tokito, *J. Am. Chem. Soc.*, 2004, **126**, 8138-8140.
31. Y. Sakamoto and T. Suzuki, *J. Org. Chem.*, 2017, **82**, 8111-8116.
32. R. H. Pawle, T. E. Haas, P. Mueller and S. W. Thomas, III, *Chem. Sci.*, 2014, **5**, 4184-4188.
33. S. A. Sharber, R. N. Baral, F. Frausto, T. E. Haas, P. Mueller and S. W. Thomas, III, *J. Am. Chem. Soc.*, 2017, **139**, 5164-5174.
34. S. A. Sharber, K.-C. Shih, A. Mann, F. Frausto, T. E. Haas, M.-P. Nieh and S. W. Thomas, *Chem. Sci.*, 2018, **9**, 5415-5426.
35. W. H. Melhuish, *J. Phys. Chem.*, 1961, **65**, 229-&.
36. M. Jean, J. Renault, P. van de Weghe and N. Asao, *Tet. Lett.*, 2010, **51**, 378-381.
37. M. A. Fox, J. A. K. Howard, J. A. H. MacBride, A. Mackinnon and K. Wade, *J. Organomet. Chem.*, 2003, **680**, 155-164.
38. D. Vonlanthen, J. Rotzler, M. Neuburger and M. Mayor, *Eur. J. Org. Chem.*, 2010, 120-133.
39. J. H. Williams, J. K. Cockcroft and A. N. Fitch, *Angew. Chem. Int. Ed.*, 1992, **31**, 1655-1657.
40. D. M. Cho, S. R. Parkin and M. D. Watson, *Org. Lett.*, 2005, **7**, 1067-1068.
41. A. Facchetti, M. H. Yoon, C. L. Stern, H. E. Katz and T. J. Marks, *Angew. Chem. Int. Ed.*, 2003, **42**, 3900-3903.
42. M. H. Yoon, A. Facchetti, C. E. Stern and T. J. Marks, *J. Am. Chem. Soc.*, 2006, **128**, 5792-5801.
43. X. Zhang, H. Yu and Y. Xiao, *J. Org. Chem.*, 2012, **77**, 669-673.

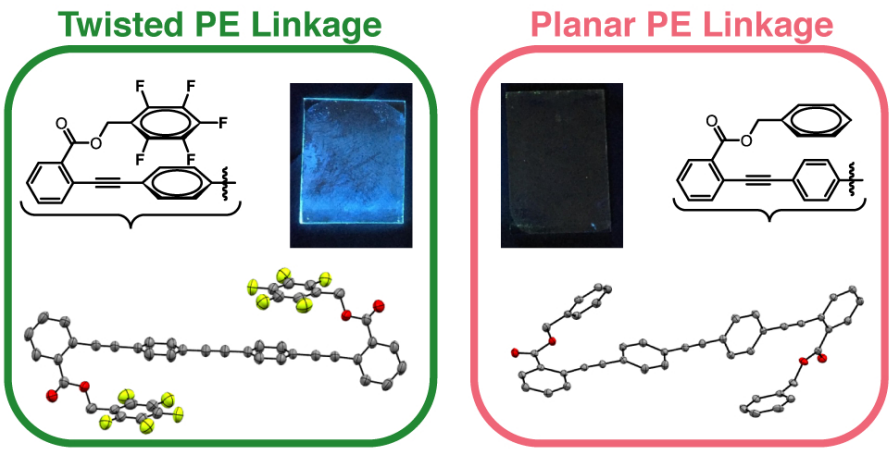
Twisted PE Linkage
Planar PE Linkage
F
F
F
F
F
O
O
O
O

TOC Text:

Intramolecular aromatic stacking of *ortho*-pentafluorobenzyl benzoate esters enables rational design of conformations of conjugated materials by programming twisted phenylene-ethynylene linkages reliably.